Wnt canonical pathway activates macropinocytosis and lysosomal degradation of extracellular proteins

Nydia Tejeda-Muñoz[a,b,1], Lauren V. Albrecht[a,b,1], Maggie H. Bui[a,b], and Edward M. De Robertis[a,b,2]

[a]Howard Hughes Medical Institute, University of California, Los Angeles, CA 90095-1662; and [b]Department of Biological Chemistry, University of California, Los Angeles, CA 90095-1662

Contributed by Edward M. De Robertis, April 2, 2019 (sent for review March 1, 2019; reviewed by Sergio P. Acebron and Stefano Piccolo)

Canonical Wnt signaling is emerging as a major regulator of endocytosis. Wnt treatment markedly increased the endocytosis and degradation in lysosomes of BSA. In this study, we report that in addition to receptor-mediated endocytosis, Wnt also triggers the intake of large amounts of extracellular fluid by macropinocytosis, a nonreceptor-mediated actin-driven process. Macropinocytosis induction is rapid and independent of protein synthesis. In the presence of Wnt, large amounts of nutrient-rich packages such as proteins and glycoproteins were channeled into lysosomes after fusing with smaller receptor-mediated vesicles containing glycogen synthase kinase 3 (GSK3) and protein arginine ethyltransferase 1 (PRMT1), an enzyme required for canonical Wnt signaling. Addition of Wnt3a, as well as overexpression of Dishevelled (Dvl), Frizzled (Fz8), or dominant-negative Axin induced endocytosis. Depletion of the tumor suppressors adenomatous polyposis coli (APC) or Axin dramatically increased macropinocytosis, defined by incorporation of the high molecular weight marker tetramethylrhodamine (TMR)-dextran and its blockage by the Na^+/H^+ exchanger ethylisopropyl amiloride (EIPA). Macropinocytosis was blocked by dominant-negative vacuolar protein sorting 4 (Vps4), indicating that the Wnt pathway is dependent on multivesicular body formation, a process called microautophagy. SW480 colorectal cancer cells displayed constitutive macropinocytosis and increased extracellular protein degradation in lysosomes, which were suppressed by restoring full-length APC. Accumulation of the transcriptional activator β-catenin in the nucleus of SW480 cells was inhibited by methyltransferase inhibition, EIPA, or the diuretic amiloride. The results indicate that Wnt signaling switches metabolism toward nutrient acquisition by engulfment of extracellular fluids and suggest possible treatments for Wnt-driven cancer progression.

macropinocytosis | arginine methylation | ESCRT | adenomatous polyposis coli | Wnt-STOP

The canonical Wnt pathway signals through stabilization of the transcriptional activator β-catenin, which is translocated into the nucleus where it binds to the TCF/LEF transcriptional factors, activating Wnt target genes (1). In the absence of Wnt, β-catenin is rapidly degraded by a destruction complex consisting of the tumor suppressor proteins Axin and adenomatous polyposis coli (APC), and the enzymes casein kinase 1 (CK1) and glycogen synthase kinase 3 (GSK3) that phosphorylate β-catenin, generating a phosphodegron that is recognized by polyubiquitin ligases leading to β-catenin degradation in proteasomes (2, 3). The Wnt growth factor binds to its cell surface coreceptors LDL receptor-related protein 6 (Lrp6) and Frizzled (Fz). Formation of this trimeric complex recruits Dishevelled (Dvl) and Axin to the plasma membrane in what is known as the Lrp6 signalosome (4, 5). These receptor complexes are then internalized into the cell and, as they enter the late endosome, are engulfed inside the intraluminal vesicles (ILVs) of multivesicular bodies (MVBs) (6). Lrp6, Fz, Axin, and Dvl are substrates of GSK3, and this key enzyme is sequestered together with the receptor complex inside MVBs. The invagination of ILVs in late endosomes is a normal occurrence during membrane trafficking and is called microautophagy, to distinguish it from macroautophagy which involves the formation of double-membrane vesicles (7). Recent results indicate that Wnt treatment strongly increases microautophagy (8).

Sequestration of GSK3 in vesicles is essential for Wnt signaling, as demonstrated by blocking MVB formation by interfering with the endosomal sorting complexes required for transport (ESCRT) machinery (6). In addition to the stabilization of β-catenin, the sequestration of GSK3 from the cytosol results in the stabilization of many other GSK3 substrate proteins (9–12) in a process designated Wnt stabilization of proteins (Wnt-STOP) (9). It has also been found that Wnt triggers arginine methylation of many proteins through the activity of protein arginine methyltransferase 1 (PRMT1) (8, 13). Arginine methylation primes the phosphorylation of certain GSK3 substrates (8, 14) and is required for canonical Wnt signaling (8). PRMT1 methylation is also required for the earliest steps of BMP and TGF-β signaling (15, 16) and is therefore emerging as an unexpected mediator of signal transduction.

Constitutive activation of the Wnt pathway is at the core of many human cancers (1, 17). The majority of colorectal cancers are initiated by loss-of-function mutations in the destruction complex component APC, resulting in increased nuclear β-catenin (18, 19). Familial adenomatous polyposis (FAP) is a disease caused by inherited heterozygous truncations in APC. Patients develop hundreds to thousands of benign polyps upon acquiring a second-hit APC loss-of-function mutation (18, 20). These benign polyps progress into colorectal cancer only after acquiring multiple additional mutations, making the initial Wnt activation a prime therapeutic target (18). Axin loss-of-function mutations are frequent in hepatocellular and many other cancers (19). RNF43 and

Significance

There is a critical need for new drugs targeting Wnt-driven diseases. For example, 80% of colorectal cancers are initiated by Wnt-activating APC mutations which then require multiple additional mutations to progress into invasive cancer. Here we present cell biological studies showing that Wnt pathway activation, or mutation of the tumor suppressors APC or Axin, greatly increased macropinocytosis. In the presence of Wnt, membrane ruffles at the plasma membrane engulfed large volumes of extracellular fluids which were channeled for degradation in lysosomes. The experiments suggest that inhibition of multivesicular body formation, methylation, or the Na^+/H^+ exchanger, may help prevent Wnt-driven cancer progression.

Author contributions: N.T.-M., L.V.A., and E.M.D.R. designed research; N.T.-M, L.V.A., and M.H.B. performed research; N.T.-M., L.V.A., and E.M.D.R. analyzed data; and N.T.-M., L.V.A., and E.M.D.R. wrote the paper.

Reviewers: S.P.A., Heidelberg University; and S.P., University of Padova.

The authors declare no conflict of interest.

[1]N.T.-M. and L.V.A. contributed equally to this work.

[2]To whom correspondence should be addressed. Email: ederobertis@mednet.ucla.edu.

This article contains supporting information online at www.pnas.org/lookup/suppl/doi:10.1073/pnas.1903506116/-/DCSupplemental.

Published online May 6, 2019.

ZNRF3 are potent transmembrane ubiquitin ligases that downregulate Lrp6 and Fz receptors, leading to increased Wnt signaling when mutated in cancers (21). Gain-of-function mutations that stabilize β-catenin (CTNNB1), or translocations leading to overexpression of R-spondin 2 or 3 (which are secreted antagonists of RNF43 and ZNRF3) also cause cancer (21, 22). Therefore, the identification of novel approaches that interfere with Wnt signaling are of considerable medical interest, and recent experiments point to endocytosis as a novel target.

In agreement with the initial discovery of the involvement of late endosomes/MVBs in GSK3 sequestration (6), recent and independent work from three different laboratories suggests that one of the fundamental functions of canonical Wnt signaling is to regulate the endocytic activity of the cell (8, 23, 24).

First, Albrecht et al. (8) reported that within minutes of Wnt3a treatment there is a striking increase in the uptake of BSA-dequenched (BSA-DQ) into lysosomes in a number of cultured cell lines. BSA-DQ is a tracer that fluoresces only after being digested by proteases within lysosomes. Wnt addition strongly increased both endocytosis and lysosomal degradation of extracellular protein (8). It was also found that the activity of protein arginine methyltransferase 1 (PRMT1) was required for the sequestration of GSK3 in MVBs and that GSK3 phosphorylation of some substrates, such as the tumor suppressor Smad4, requires prior methylation by PRMT1. As documented in the movies in ref. 8, NIH 3T3 fibroblasts did not normally digest extracellular proteins, but were induced to do so within minutes of the addition of Wnt3a.

Second, Saito-Diaz et al. (23) discovered that the tumor suppressor APC normally dampens Wnt/β-catenin signaling by repressing the clathrin-dependent endocytic pathway. APC is a microtubule-binding protein (25, 26) that also binds to clathrin and its adaptor AP2 (23). APC knockdown induced the internalization of the Lrp6 receptor and triggered signaling in the absence of Wnt ligand (23). Although changes in the endocytosis of exogenous proteins were not examined in that study, the inhibition of the APC deficiency effects by blocking clathrin suggested that a main effect of the loss of APC was to increase clathrin-coated vesicle endocytosis (23).

Third, Redelman-Sidi et al. (24) analyzed the role of Wnt signaling through a different approach, starting with the phagocytosis of *Bacillus* Calmette-Guérin (BCG), which is used as a bacterial treatment for bladder cancer. They found that siRNAs that increase Wnt signaling (such as knockdown of Kremen1 or DKK1) resulted in increased BCG uptake due to an increase in macropinocytosis. Phagocytosis and macropinocytosis are actin-driven processes that share many common elements (27, 28). Pinocytosis is drinking by cells while phagocytosis is eating by cells. Pinocytosis was first identified by Lewis (29), who followed the cellular uptake of globules of fluid visible under the light microscope. However, with the advent of electron microscopy many other types of micropinocytosis—such as caveolae and coated vesicle endocytosis—were revealed (30–32). The term macropinocytosis is currently employed (instead of simply pinocytosis as was previously used) to designate endocytosis of extracellular fluid in vesicles of a diameter in excess of 0.2 μm (33, 34). Tetramethylrhodamine-dextran with a hydrated diameter of 200 nm (TMR-dextran 70 kDa) uptake and its inhibition by amiloride derivatives such as ethylisopropyl amiloride (EIPA) constitute the modern gold standard for macropinocytosis (34, 35). Activation of Wnt signaling triggered macropinocytosis in a number of colorectal cancer cell lines with loss of function of APC (24). In addition, an increase in bacterial phagocytosis and macropinocytosis into enterocytes was observed, using an in vivo mouse model of early colorectal cancer involving inducible APC shRNA (24).

In this study, we present further analysis of our discovery of Wnt-induced endocytosis and degradation of extracellular proteins in lysosomes (8). The increase in protein uptake was caused by macropinocytosis, in which circular membrane ruffles accompanied by F-actin reorganization folded over large amounts of extracellular fluid within minutes of Wnt3a treatment. Activity of PRMT1 and the ESCRT machinery were required for Wnt-induced macropinocytosis. Endocytic uptake of TMR-dextran 70 kDa was inhibited by EIPA and amiloride (a diuretic commonly used in the clinic that inhibits plasma membrane Na^+/H^+ exchangers). A number of gain-of-function treatments, such as the overexpression of Dishevelled (Dvl), caused a marked increase of endocytosis and lysosomal degradation of BSA-DQ. In a loss-of-function situation, Axin or APC siRNA increased macropinocytosis, in agreement with ref. 24. The colorectal carcinoma cell line SW480 in which APC is mutated (36, 37), but not SW480APC in which full-length APC was restored (37), displayed constitutive macropinocytosis, nuclear β-catenin accumulation, and high levels of extracellular albumin digestion. Nuclear β-catenin accumulation in SW480 cells, which is controlled by Wnt signaling, was inhibited by amiloride, EIPA, and methylation inhibition. The emerging connection between Wnt signaling, arginine methylation, lysosomal trafficking, and macropinocytosis suggests new therapeutic possibilities to prevent progression of cancers initiated by activation of the Wnt pathway.

Results

Wnt Treatment Triggers Macropinocytosis in Cultured Cells. Wnt3a induced large vesicular structures in HeLa cells within 20 min of addition, and in situ proteinase K protection assays (8) indicated that these vesicles contained GSK3 sequestered from the cytosol (Fig. 1 *A–D*, quantitated in *SI Appendix*, Fig. S1). Concomitantly, large rearrangements of cortical F-actin, visualized by phalloidin staining, took place at the cell cortex, appearing to envelop large regions of plasma membrane (Fig. 1 *E* and *F*, arrowheads). These structures were reminiscent of the events taking place during macropinocytosis, which is an actin-driven process that does not involve clathrin (30, 38). To examine actin remodeling in real time, we used cells transfected with the F-actin tracer LifeAct (Gonagen) (Fig. 1 *G* and *H* and Movie S1). SW480APC cells, which responded strongly to Wnt signaling (*SI Appendix*, Fig. S2), revealed that Wnt3a induced extensive rearrangements of filamentous actin at the leading edge lamellipodium, forming transient membrane ruffles that tended to encircle extracellular fluid, delimiting large vesicles indicative of macropinocytosis (Fig. 1*H*, arrowheads).

To confirm that Wnt indeed induced macropinocytosis, 3T3 cells were treated with TMR-dextran 70 kDa (35) for 1 h. Wnt3a caused a large increase in dextran uptake, which was blocked by the Na^+/H^+ exchanger inhibitor EIPA (Fig. 1 *I–L* and *SI Appendix*, Fig. S1*D*). Importantly, macropinocytosis of TMR-dextran was independent of new protein synthesis since it also took place in Wnt-treated cells preincubated with cycloheximide (*SI Appendix*, Fig. S3).

We previously reported that PRMT1 was required for Wnt signaling (8, 13). To determine whether the PRMT1 enzyme plays a role in macropinocytosis, NIH 3T3 cells were transfected with previously validated control or PRMT1 siRNA (8). It was found that PRMT1 depletion blocked Wnt-induced macropinocytosis (Fig. 1 *M–P*). Taken together, the results indicate that canonical Wnt rapidly induces cortical actin rearrangements and macropinocytosis, in a process that requires PRMT1 and is independent of protein synthesis.

Activation of Wnt Pathway Components Increases BSA Digestion in Lysosomes. Next, we tested whether activation of the Wnt pathway increased endocytosis of BSA-DQ independently of the presence of the ligand. Dishevelled (Dvl) overexpression is an activator of canonical Wnt signaling (39). HeLa cells transfected with xDvl-myc (40) contained prominent vesicles of endocytosed

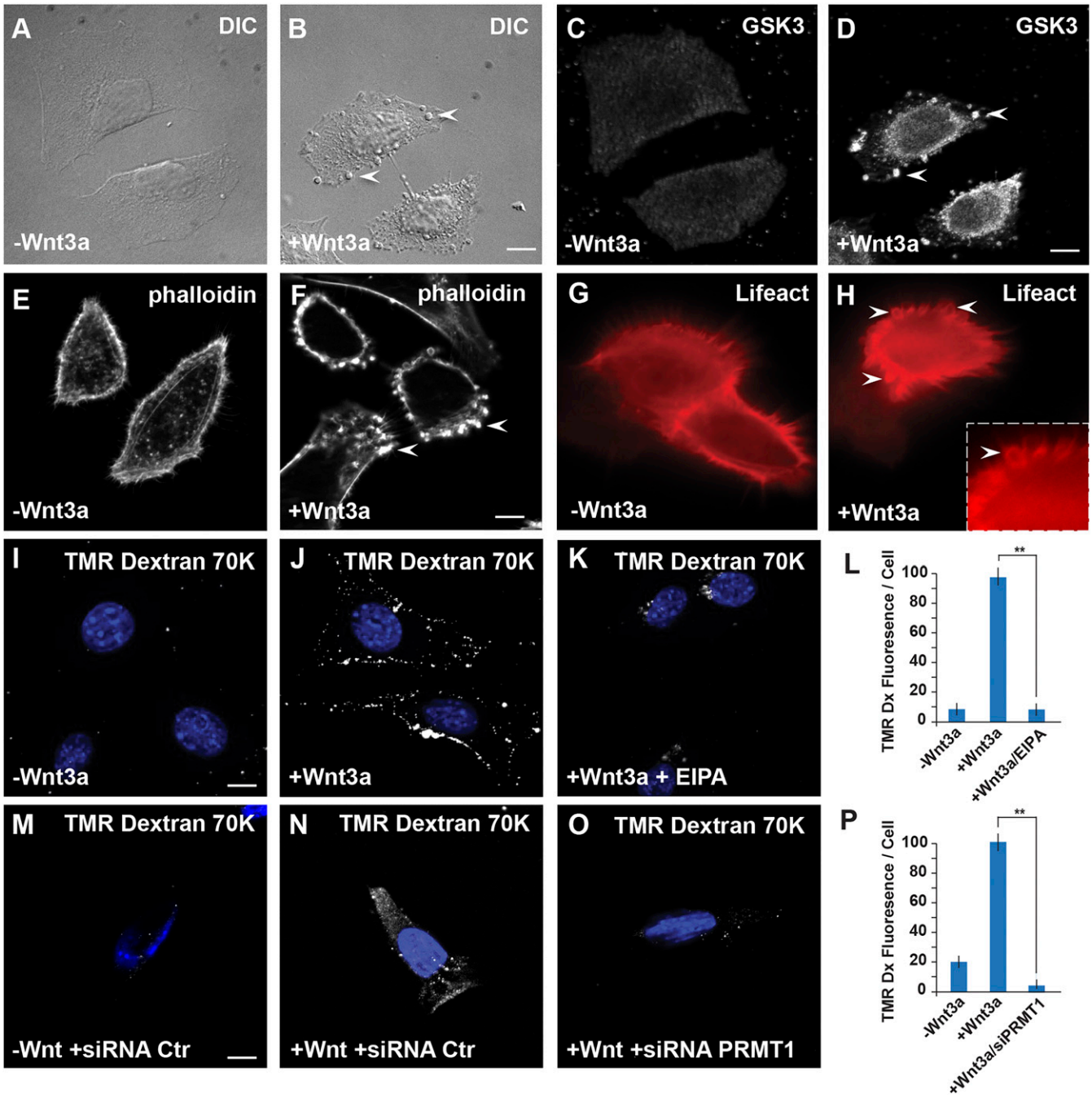

Fig. 1. Wnt signaling induces the formation of large vesicles generated by macropinocytosis. (*A* and *B*) Phase contrast images of HeLa cells showing that 20 min of Wnt treatment induces the formation of large vesicle-like structures (arrowheads). (*C* and *D*) In situ proteinase K protection assay (8) showing that GSK3, a key enzyme in the Wnt pathway, is translocated from the cytoplasm into large MVBs following Wnt3a treatment for 20 min. (*E* and *F*) Wnt3a induces rearrangement of the cortical F-actin cytoskeleton visualized by phalloidin staining; note that actin surrounds large vesicles 20 min after stimulation of HeLa cells with Wnt3a. (*G* and *H*) Still images from Movie S1 showing that F-actin (visualized with transfected LifeAct) at the leading edge lamellipodium forms macropinocytotic vesicles within 20 min of treating SW480APC cells with Wnt. (*I–L*) Wnt induces macropinocytosis in NIH 3T3 cells, assayed by uptake of TMR-dextran 70 kDa and inhibition with the amiloride derivative EIPA. (*M–P*) Depletion of the enzyme PRMT1 (which is essential for the activation of the Wnt pathway), but not control scrambled siRNA (8), blocked macropinocytosis in NIH 3T3 cells. $^{**}P < 0.01$. (Scale bars, 10 μm.)

and digested BSA-DQ, while untransfected cells (outlined by stippled lines) had only low levels of endocytosis (Fig. 2 *A* and *B*). Overexpression of the Wnt receptor Fz8 (41) also increased endocytosis of BSA-DQ added to the culture medium of 3T3 cells (Fig. 2 *C* and *D*). A very potent activator of Wnt signaling is a fusion protein consisting of the DIX domain of Dvl fused to the Lrp6 cytoplasmic tail (42). Cells transfected with Dvl DIX > Ctail-GFP displayed increased BSA endocytic vesicles (Fig. 2 *E* and *F*). This construct has a very useful mutant control in which changing two amino acids in the DIX domain eliminates Wnt pathway biological activity and binding to vesicles (39, 42). Transfected mutant control DIX > Ctail-GFP-M2 was expressed, but failed to increase endocytosis (compare Fig. 2 *E* and *G*), indicating that BSA-DQ endocytosis was specific to Wnt signaling.

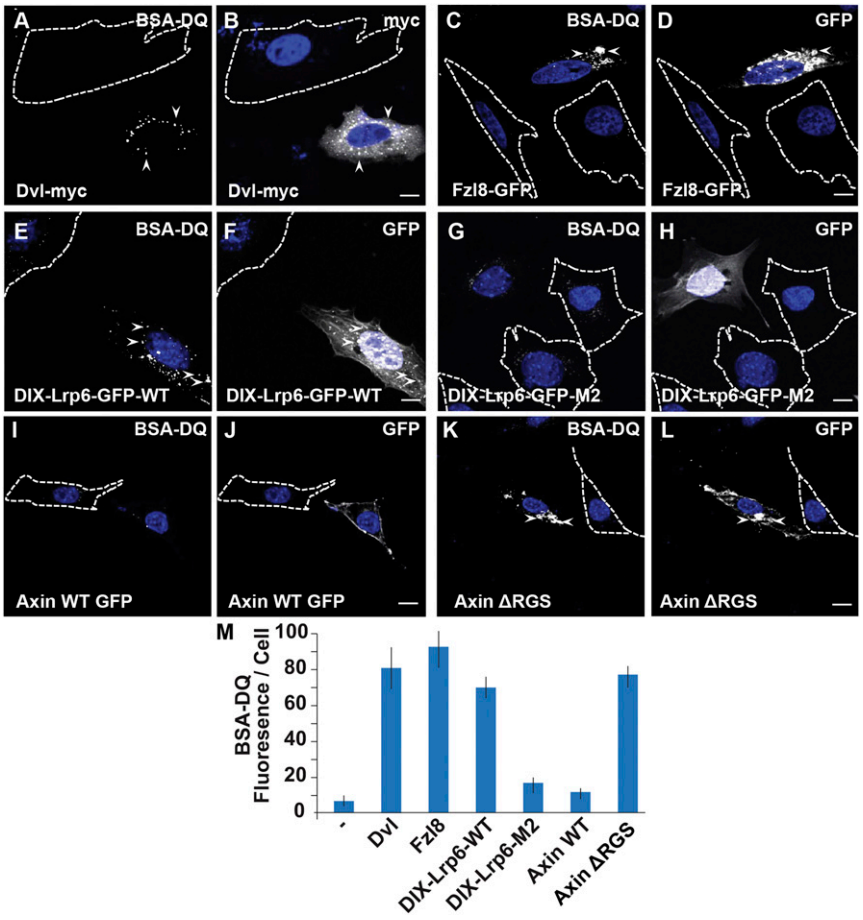

Fig. 2. Endocytosis and lysosomal degradation of BSA-DQ is increased by transfection of DNA constructs that activate the Wnt pathway. Untransfected cells serve as controls and are demarcated by a stippled line. (*A* and *B*) Fluorescence microscopy images showing that Dvl-myc overexpression increases endocytosis of BSA-DQ and degradation in HeLa cells (arrowheads); note that the untransfected cell has less BSA-DQ fluorescence than the transfected cell. (*C* and *D*) Overexpressed Wnt receptor Fz8 triggers BSA-DQ endocytosis (arrowheads). (*E* and *F*) Transfection of the fusion protein DIX-Lrp6-GFP, a strong activator of the Wnt pathway, triggered increased BSA-DQ endocytosis (arrowheads). (*G* and *H*) The control DIX-LRP6-GFP-M2 mutant, which has two mutations in the DIX domain of Dvl and is inactive in Wnt signaling (42), did not increase endocytosis. (*I* and *J*) Axin, an inhibitor of the Wnt pathway, did not affect endocytosis. (*K* and *L*) Dominant-negative Axin ΔRGS increased endocytosis of BSA-DQ (arrowheads). (*M*) Quantification of the activation of Wnt signaling by overexpression of a multiple-transfected DNA construct. Fluorescence per cell was quantified, as described in *Materials and Methods* analyzing a minimum of 25 transfected cells per condition. Untransfected NIH 3T3 cells are indicated by the minus (–) label. The M2 mutant DIX-Lrp6Ctail-M2 and Axin wild-type serve as negative controls that did not increase Wnt signaling nor endocytosis. (Scale bars, 10 μm.)

Axin is a component of the destruction complex that normally inhibits Wnt signaling. Its overexpression in transfected cells did not appear to affect endocytosis (Fig. 2 *I* and *J*). A dominant-negative form has been generated by deleting its amino terminal RGS domain (Axin-ΔRGS) (43). Cells transfected with dominant-negative Axin-ΔRGS showed abundant extracellular BSA utilization (Fig. 2 *K* and *L*). These experiments, quantitated in Fig. 2*M*, demonstrate that activation of the Wnt pathway by multiple mechanisms resulted in increased endocytosis and digestion of BSA in lysosomes.

Loss of Function of APC or Axin Increases Macropinocytosis. To test in a loss-of-function situation whether the activation of macropinocytosis was a generalized phenomenon, we used knockdown of Axin or APC using previously validated siRNA reagents (6, 23). We found that depletion of Axin or APC greatly stimulated macropinocytosis of TMR-dextran 70 kDa and uptake and degradation of BSA-DQ in lysosomes in NIH 3T3 cells (Fig. 3 *A*–*D* and *SI Appendix*, Fig. S4). APC depletion led to the translocation of the cytosolic enzymes PRMT1 and GSK3 to vesicles in HeLa cells (Fig. 3 *E*–*J*), as is known to occur in Wnt3a-treated cells (8).

We next tested whether the colorectal cancer cell line SW480, which carries loss-of-function mutations in APC, had increased endocytosis. As a control, we used the SW480APC cells in which full-length APC was stably restored by Faux et al. (37). Both cell lines were subjected to the same selection procedures, and therefore provided an ideal situation since the only difference between them is the presence or absence of APC. SW480 cells, but not SW480APC cells, had extremely high constitutive endocytic activity, becoming engorged with the BSA in lysosomes within 30 min of BSA-DQ addition (Fig. 3 *K*–*N* and Movie S2, quantitated in Fig. 3*S*). The amounts of serum proteins utilized in the absence of APC must be very high since the BSA-DQ tracer was added at 5 μg/mL, while the 10% serum used in the culture medium contains 3.5–5 mg/mL of BSA. This indicates that APC deletion triggers a major shift in nutrient acquisition by colorectal carcinoma cells. The increased uptake by APC mutation was due to macropinocytosis, as indicated by incubation for 1 h with TMR-dextran 70 kDA (Fig. 3 *O*–*R*, quantitated in Fig. 3*T*). These experiments indicate that loss of the tumor suppressors Axin or APC causes major changes in cell nutrition, triggering a large increase in macropinocytosis followed by degradation of extracellular protein in lysosomes.

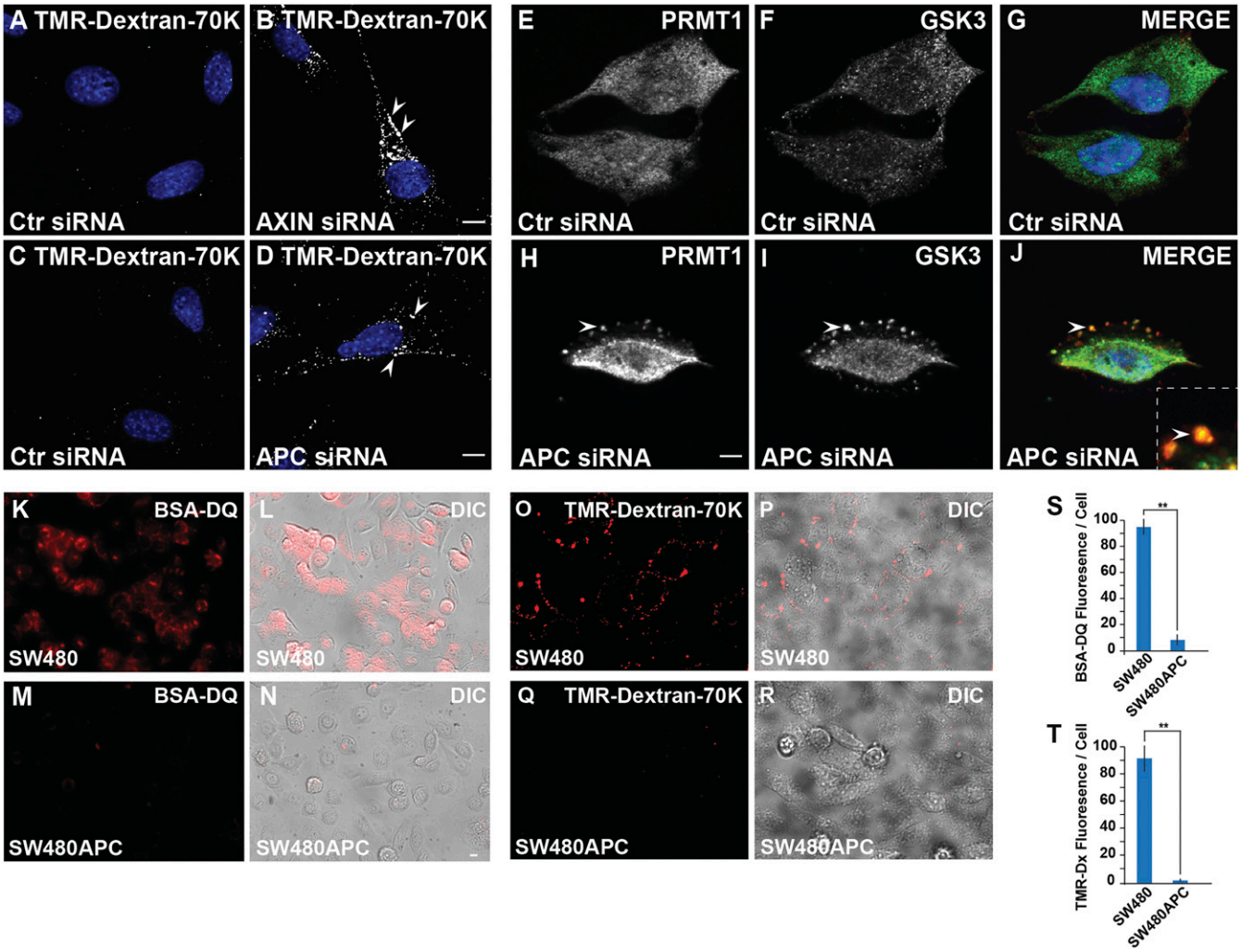

Fig. 3. Loss of function of the tumor suppressors Axin or APC trigger macropinocytosis of high molecular weight TMR-dextran 70 kDa, GSK3 and PRMT1 translocation to vesicles, and increased degradation of extracellular BSA protein in lysosomes. (*A–D*) Depletion of Axin or APC with siRNA triggered an increase in macropinocytosis marked by TMR-dextran 70 kDa in NIH 3T3 cells. Note that although Axin and APC are components of the β-catenin destruction complex, they also function as repressors of macropinocytosis. (*E–J*) APC induces localization of PRMT1 and GSK3 in vesicles in HeLa cells; GSK3 and PRMT1 sequestration are essential steps in canonical Wnt signaling. (*K–N*) Still images from Movie S2 showing that the colon cancer cell line SW480 had high BSA-DQ utilization within 30 min of addition, which was greatly reduced when full-length APC was restored in an isogenic cell line (SW480APC). (*O–R*) Similar experiment using the macropinocytosis tracer TMR-dextran 70 kDa. (*S*) Quantification of BSA-DQ digestion per SW480 or SW480APC cell. (*T*) Quantification of macropinocytosis of TMR-dextran 70 kDa in SW480 cells and its inhibition by restoration of APC. $^{**}P < 0.01$. (Scale bars, 10 μm.)

The ESCRT Machinery Is Required for Macropinocytosis and β-Catenin Nuclear Localization in APC Mutant Cells. Canonical Wnt signaling requires the sequestration of GSK3 in the intraluminal vesicles of MVBs/late endosomes. Treatments that interfere with the ESCRT machinery block β-catenin stabilization and Wnt signaling (6). To test whether the ESCRT machinery was required for Wnt-induced macropinocytosis, we used a dominant-negative form of the Vps4 ATPase caused by a point mutation (Vps4-EQ) that inhibits MVB formation (44). SW480 cells transfected with wild-type Vps4-WT-GFP had unchanged uptake of TMR-dextran 70 kDa (Fig. 4 *A–C*, transfected cell indicated by a stippled rectangle), whereas macropinocytosis was inhibited in cells transfected with Vps4-EQ-GFP (Fig. 4 *D–G*, compare transfected cells in Fig. 4 *A* and *D*). This indicates that MVBs/late endosomes are required for the trafficking of macropinosomes.

SW480 cells, in which Wnt is constitutively active, have high levels of β-catenin. While Vps4-WT-GFP did not affect β-catenin levels, Vps4-EQ-GFP transfected cells had greatly reduced nuclear and cytoplasmic β-catenin levels (Fig. 4 *H–N*, compare stippled rectangles in Fig. 4 *H* and *K*). When the transfection efficiency of SW480 cells was optimized (by starving the cells from serum for 12 h followed by transfection with Lipofectamine 3000), the decrease in β-catenin levels caused by ESCRT inhibition was also detected in Western blots (Fig. 4*O*). We conclude that MVB formation, which is integral to Wnt signaling, is required both for macropinocytosis and for nuclear β-catenin accumulation in APC mutant cells.

Inhibition of Macropinocytosis May Provide New Therapeutic Opportunities. SW480 cells have robust macropinocytosis and nuclear β-catenin localization (Fig. 5*A*) caused by the loss of APC. As shown earlier, Wnt-induced macropinocytosis of TMR-dextran 70 kDa required the activity of the Na^+/H^+ exchanger (Fig. 1 *I–L*). SW480 cells have very high constitutive plasma membrane motility, which was decreased by the amiloride derivative EIPA (Movie S3). We found that nuclear β-catenin levels were significantly reduced in SW480 colorectal cancer cells after 2 h of treatment with 40 μM EIPA or 2 mM amiloride

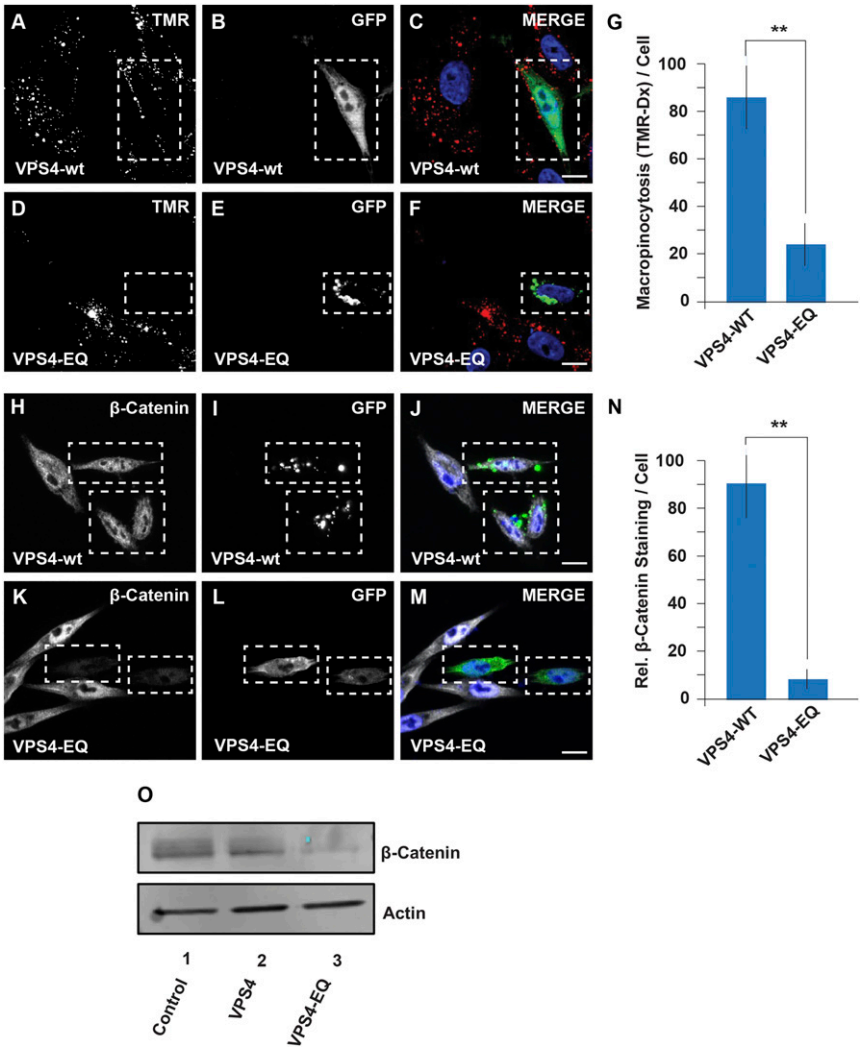

Fig. 4. The ESCRT machinery protein Vps4 is required for macropinocytosis and β-catenin nuclear accumulation in SW480 colorectal carcinoma cells. Vps4 is an ATPase, and the point mutation Vps4-EQ serves as a dominant-negative that prevents ESCRT machinery from recycling, therefore blocking microautophagy in late endosomes (44). (*A–C*) SW480 cells were transfected with Vps4-GFP and treated with the macropinocytosis marker TMR-dextran for 1 h; note that the cell which was transfected (indicated by a stippled square) had normal amounts of macropinocytosis. (*D–F*) Overexpression of dominant-negative Vps4-EQ blocked macropinocytosis of TMR-dextran, indicating that the ESCRT machinery function is required for macropinocytosis. (*G*) Quantification of the inhibitory effect of blocking the ESCRT machinery in transfected SW480 cells. (*H–J*) The SW480 cell line presents strong constitutive β-catenin staining that was unaffected by the overexpression of Vps4 (transfected cells indicated by stippled boxes). (*K–M*) Levels of β-catenin were greatly reduced in SW480 cells transfected with the dominant-negative Vps4-EQ (indicated by rectangles), but not in untransfected cells. (*N*) Quantification of the effect on β-catenin levels of blocking the ESCRT machinery in transfected cells. (*O*) Western blot showing that endogenous levels of β-catenin were reduced in dominant-negative Vps4-EQ transfected SW480 cells; actin serves as a loading control. $^{**}P < 0.01$. (Scale bars, 10 μm.)

(Fig. 5 *A–F*, nuclear/cytoplasmic ratios quantitated in Fig. 5*G*). Since Wnt-induced macropinocytosis requires PRMT1, we also tested whether the constitutive nuclear localization of β-catenin was affected by the competitive methylation inhibitor adenosine-2′,3′-dialdehyde (Adox) (45). After incubation with 20 μM Adox for 24 h, a marked decrease in nuclear β-catenin levels was observed in SW480 cells (Fig. 5*H* and *SI Appendix*, Fig. S5). Finally, we examined β-catenin transcriptional activity using β-catenin activated reporter (BAR) Luciferase/Renilla reporter assays. Treatment with the Na^+/H^+ exchanger inhibitors EIPA or amiloride inhibited Wnt signaling activity in transiently transfected SW480 cells (Fig. 5*I*). In addition, Wnt3a signaling in HEK293T cells stably expressing BAR and Renilla reporters (8) was inhibited by EIPA or amiloride (Fig. 5*J*). These findings are of potential medical interest as amiloride has been used as a human diuretic for decades, and new PRMT1 inhibitors are being developed (46).

Discussion

Wnt Signaling and Macropinocytosis. This study was prompted by our observation that Wnt treatment induced a rapid increase in the endocytosis and degradation of BSA-DQ in lysosomes (8). The large size of the vesicular structures formed (>200 nm) suggested the induction of macropinocytosis and rapid trafficking into the endosomal machinery. It was found that the actin cytoskeleton at the leading edge of cultured cells displayed Wnt-induced rearrangements with circular ruffling membranes suggesting macropinocytosis. We confirmed that macropinocytosis was indeed rapidly increased by Wnt3a using high molecular weight TMR-dextran 70 kDa and blocking its uptake by a Na^+/H^+ exchanger inhibitor EIPA (35). Macropinocytic vesicles matured into MVBs/late endosomes that sequestered cytosolic GSK3 and PRMT1 by microautophagy, which are required for canonical Wnt signaling (6, 8). Overexpression of multiple activators of the Wnt

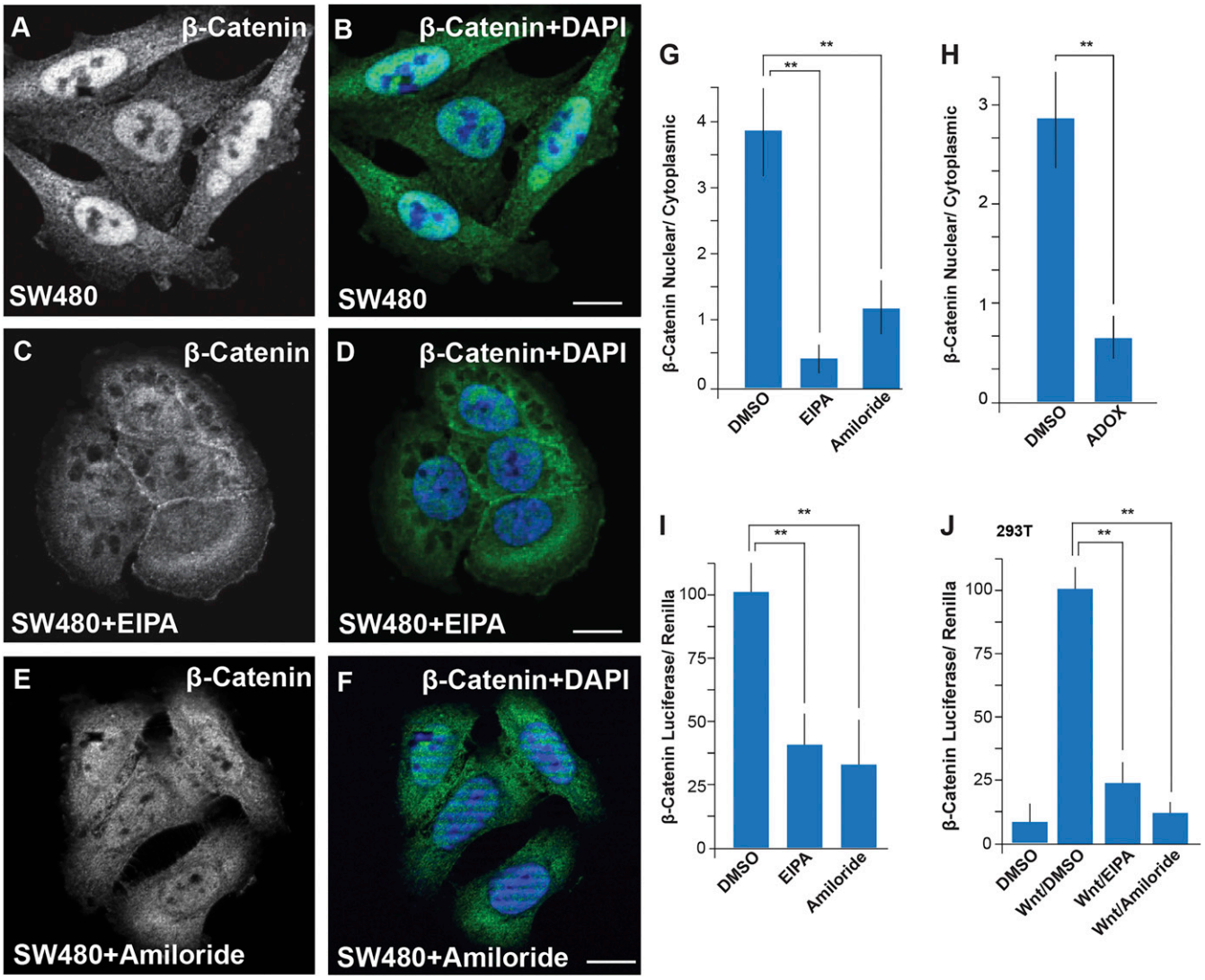

Fig. 5. Inhibitors of macropinocytosis or methylation decrease constitutive nuclear β-catenin accumulation in the colorectal cancer cell line SW480. (*A–F*) A marked reduction in nuclear β-catenin levels was caused by inhibiting macropinocytosis with EIPA or amiloride for 2 h. These agents inhibit macropinocytosis by blocking the plasma membrane Na^+/H^+ exchanger, resulting in acidification of cortical cytoplasm and inhibition of actin remodeling; amiloride is a diuretic that has been used in humans for over 50 y. (*G*) Quantification of β-catenin nuclear to cytoplasmic ratios, which were significantly reduced by EIPA or amiloride treatment (*Materials and Methods*). (*H*) Nuclear/cytoplasmic of β-catenin ratios were significantly reduced in SW480 cells treated with the methylation inhibitor Adox; corresponding immunofluorescence images are shown in *SI Appendix*, Fig. S5. (*I*) EIPA or amiloride treatment inhibited BAR Luciferase/Renilla activity in transiently transfected SW480 cells. (*J*) The macropinocytosis inhibitors EIPA or amiloride reduced Wnt3a signaling in HEK293T cells stably transfected with BAR/Renilla reporters. $^{**}P < 0.01$. (Scale bars, 10 μm.)

pathway—such as Dishevelled, Fz8, Dvl DIX > Ctail-GFP and dominant-negative Axin-ΔRGS—strongly induced BSA-DQ endocytosis and degradation in lysosomes. Knockdown of Axin1 or APC, proteins that normally repress Wnt/β-catenin signaling, also increased macropinocytosis. The SW480 colorectal cancer cell line, which has APC mutations (37) was very active in macropinocytosis and subsequent lysosomal BSA degradation, and these activities were suppressed by restoration of full-length APC. From these results canonical Wnt emerges as a major regulator of extracellular nutrient acquisition and digestion in lysosomes.

As this work was in progress, two other studies appeared that strongly supported the role of Wnt in endocytosis regulation. APC knockdown caused Lrp6 internalization and Wnt signaling via a clathrin-mediated pathway (23). In another study, it was found that siRNAs that increased Wnt signaling—such as DKK1, Kremen1, Naked1, APC, and Axin1—promoted phagocytosis and macropinocytosis (24). Macropinocytosis and phagocytosis are evolutionarily conserved processes (28). Importantly, it was also shown in an in vivo mouse colon cancer model that bacterial uptake into enterocytes is increased by APC shRNA and blocked by EIPA (24). Translocation of bacterial microbiota into colorectal tumors, with its resulting inflammation, has been proposed to promote oncogenesis (47). The results presented here fundamentally agree with refs. 23 and 24, and extend their findings. We now show that arginine methylation by PRMT1 is a regulator of macropinocytosis, that the ESCRT machinery is required for macropinocytosis, that Wnt3a triggers macropinocytosis within minutes in the absence of new protein synthesis, and that amiloride inhibits the constitutive nuclear β-catenin accumulation specifically caused by APC mutation in a colorectal cancer cell line.

The mechanism by which loss of function of the β-catenin destruction complex components APC and Axin1 trigger macropinocytosis remains a mystery. APC binds to the plus end of

microtubules at the leading edge or lamellipodium of the cell (25, 48). During macropinocytosis, actin-driven circular ruffles appear and enclose extracellular fluid. Wnt signaling is a receptor-mediated process that requires binding Lrp6 and Fz (1). Endocytosis of the receptor complex occurs either through caveolin or clathrin micropinocytosis (49, 50). In the case of APC knockdown, it is clear that receptor-mediated endocytosis is entirely dependent on clathrin-mediated endocytosis (23). However, macropinocytosis is a clathrin-independent process (30).

In the model depicted in Fig. 6, we propose that Lrp6/Fz/Wnt/Dvl signalosomes (4) are first internalized by receptor-mediated micropinocytosis and that this, by an as yet unknown molecular mechanism, subsequently triggers actin polymerization, membrane ruffling, and macropinocytosis. Both types of vesicles rapidly coalesce into common MVBs that sequester GSK3 and PRMT1 and traffic ingested extracellular macromolecules into lysosomes. Growth factor-induced macropinocytosis can be traced back to classical studies by Cohen and coworkers (51) with ferritin-labeled epidermal growth factor (EGF). EGF receptor-mediated endocytosis took place initially via coated pits and micropinocytic-coated vesicles of less than 100 nm that were rapidly incorporated into the intraluminal vesicles of MVBs by microautophagy (51). In addition, EGF stimulated a transient population of large macropinocytic vesicles of 200–1,000 nm that engulfed large amounts of horseradish peroxidase (HRP) by nonreceptor-mediated endocytosis and lasted for only 15 min (52). The macropinocytic vesicles then fused with the coated vesicle-derived MVBs (51, 52). Since these groundbreaking findings, a large number of receptor tyrosine kinases (RTKs) have been found to transiently activate macropinocytosis when stimulated (30, 53).

Wnt in Metabolism and Cancer. Macropinocytosis provides an efficient way of obtaining nutrients through the degradation of concentrated packages of amino acids in the form of proteins and sugars from glycosylated proteins. The concentration of protein building blocks in plasma is much greater than that of free amino acids (54). Macrophages, in which macropinocytosis is constitutive, drink prodigious amounts of fluid, of up to one-third of the cell volume per hour (29). Therefore, if macropinosome contents were efficiently channeled into lysosomes by Wnt, large amounts of nutrients should become available (ref. 8, this study).

In pancreatic cancers with activating mutations of the Kras oncogene, a key feature is that metabolism is reprogrammed by constitutive macropinocytosis (34, 54). It is also known that canonical Wnt signaling induces a shift toward aerobic glycolysis, known as a Warburg effect, through β-catenin transcriptional induction of pyruvate dehydrogenase kinase 1 (55, 56). Glycolytic metabolism is maximal in the crypts of the intestine, where stem cells reside (57). Wnt signaling is high in intestinal stem cells and, interestingly, PRMT1 levels are also high (1, 58). Glycolytic metabolism is a well-known hallmark of cancer (59) and it is possible that macropinocytosis by Wnt pathway or Ras-activating mutations will contribute to this effect. Whether glucose levels ingested by macropinocytosis would be sufficient to significantly affect metabolism remains unknown. In the case of the amoeba Chaos chaos, which does not have significant glucose membrane transporters, induction of macropinocytosis intriguingly results in increased radioactive glucose consumption (60). Together with its effect on cell growth and protein stabilization (Wnt-STOP) (9, 61), canonical Wnt signaling is emerging as a major regulator of nutrient acquisition with particular relevance to stem and cancer cell biology.

As indicated in Fig. 6, the flux of plasma membrane triggered by macropinocytosis may help propel the rapid increase in MVB formation after Wnt3a treatment, reported previously (8). We can also expect that during the progression of tumors initiated by Wnt pathway activation there may be synergistic effects at the level of macropinocytosis with other oncogenic mutations—such as Ras, RTKs, PI3K, and loss of PTEN (62–64), which might be targeted by amiloride. In conclusion, basic studies in the cell biology of Wnt signaling implicating macropinocytosis, PRMT1, and the ESCRT machinery suggest possible therapeutic avenues for Wnt-driven diseases.

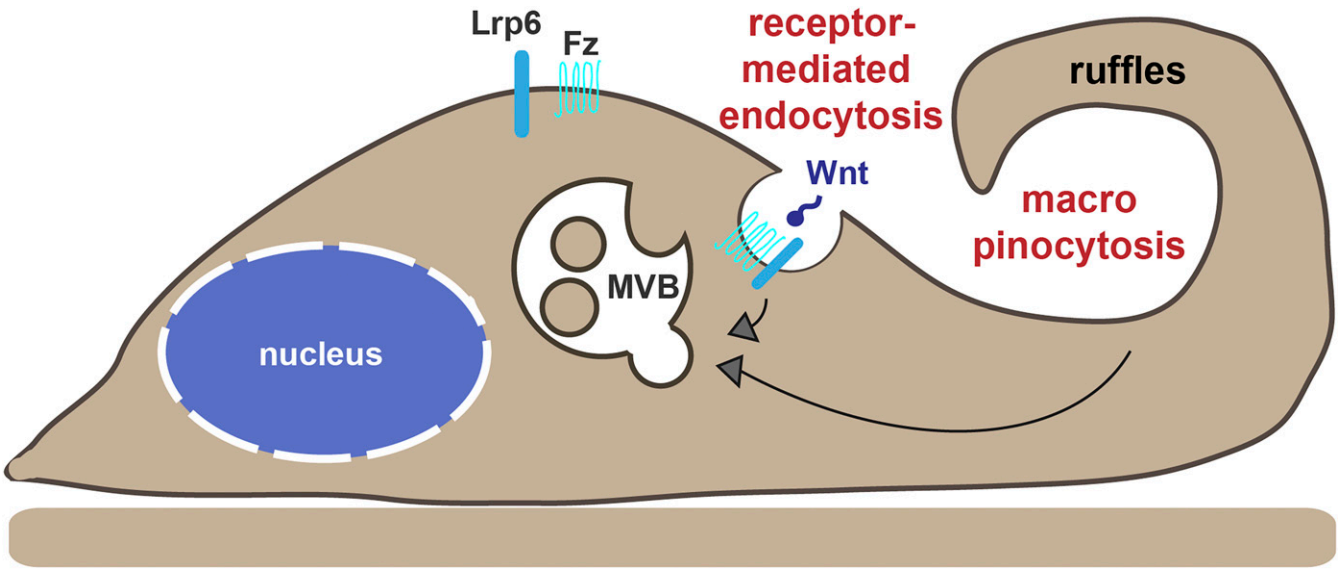

Fig. 6. Model of the effects of the growth factor Wnt in receptor-mediated endocytosis (micropinocytosis) and in receptor-independent endocytosis of proteins from extracellular fluids (macropinocytosis). The Wnt coreceptors Lrp6 and Fz are incorporated into receptor-mediated small microendocytic vesicles, triggering an as yet unknown signal that causes actin cytoskeleton remodeling in the lamellipodium at the leading edge of the cell, forming membrane ruffles and macropinocytic cups that engulf large amounts of the surrounding liquid. Both types of endosomes fuse into common MVBs/late endosomes that contain GSK3 and PRMT1 and require the ESCRT machinery for their formation. In the presence of Wnt, BSA incorporated by macropinocytosis is channeled to degradation in lysosomes, providing a source of nutrition for cells in which Wnt signaling is activated. The recycling of membrane from macropinocytic vesicles may help drive the considerable increase in microautophagy observed in MVBs/late endosomes shortly after Wnt treatment (8).

Materials and Methods

Antibodies and Reagents. Antibody against GSK3 was obtained from BD Biosciences (610201) and used for immunostaining (1:500) and Western blot (1:1,000); β-catenin mouse monoclonal was from Santa Cruz Biotechnology (sc-7963, 1:1,000); PRMT1 mouse monoclonal antibody was from Santa Cruz (sc-59648, 1:500); and actin antibody was from Santa Cruz Biotechnology (sc-58673, 1:1,000). Secondary antibodies coupled to infrared dyes [IRDye 680 (926-68072) and IRDye 800 (926-32213)] at 1:3,000 (LI-COR) were used for Western blots and analyzed with the LI-COR Odyssey System. Secondary antibodies for immunostaining (1:500) were from Jackson ImmunoResearch Laboratories, Inc (715546150, 711166152) (8). LifeAct plasmid DNA was purchased from Gonagen to visualize the F-actin cytoskeleton. To measure fluid-phase uptake through macropinocytosis, TMR-dextran 70 kDa, lysine fixable, was used (D1818; Thermo Fisher Scientific) at 1 mg/mL. To measure lysosomal proteolytic activity, BSA-DQ (D-12051, Thermo Fisher Scientific) was used at 5 μg/mL. The siRNA targeting Axin1 ON-TARGETplus SMARTpool was from Thermo Fisher Scientific L-009625 (6). APC was depleted using a mixture of two siRNAs (23). The arginine methyl-inhibitor Adox was from MilliporeSigma (A7154; 20 μM). Wnt3a protein was purchased from PeproTech (315-20) and used at 100 ng/mL. Inhibitors of macropinocytosis were obtained from Sigma-Aldrich: 5-(*N*-ethyl-*N*-isopropyl) amiloride (A3085) and amiloride hydrochloride (BP008). The optimal concentrations for inhibition of macropinocytosis in cultured cells have been determined previously to be 2 mM for amiloride (65) and 40 μM for EIPA (35) and were the concentrations used here. We tested cell viability up to 4 mM amiloride or 80 μM EIPA using a Vi-Cell Beckman-Coulter Viability Analyzer in HEK293 cells and found no effect on cell viability after 24 h.

Tissue Culture and Transfection. HeLa (ATCC, CRL-2648) or NIH 3T3 were cultured in DMEM supplemented with 10% FBS (Gibco), 1% penicillin/streptomycin, and 1% glutamine. SW480 and SW480APC were grown in DMEM F-12 supplemented with 5% FBS, antibiotics, and 2 mM glutamine. Cells were cultured at 37 °C in 5% CO_2. DNA constructs were transfected with Lipofectamine 3000 for 24 h. For RNAi depletion experiments, cells were transfected with siRNA 72 h earlier.

Immunostainings and Western Blots. HeLa, NIH 3T3, SW480, or SW480APC cells were grown on circular coverslips, fixed with 4% paraformaldehyde (Sigma, P6148) for 15 min, permeabilized with 0.2% Triton X-100 in Dulbecco's PBS (DPBS) (Gibco) for 10 min, and blocked with 5% goat serum and 0.5% BSA in DPBS for 1 h. Primary antibodies were added overnight at 4 °C. Slide chambers were washed 10 min three times with DPBS, and secondary antibodies applied for 1 h at room temperature. After three additional washes with DPBS, chambers were removed and coverslips mounted with Fluoroshield Mounting Medium with DAPI (ab104139). Immunofluorescence was analyzed and photographed using a Zeiss Imager Z.1 microscope with Apotome. For Western blots, cells were lysed with RIPA buffer containing 0.1% Nonidet P-40, 20 mM Tris/HCl pH 7.5, 10% glycerol, together with protease (Roche, 04693132001) and phosphatase inhibitors (Calbiochem, 524629).

Image Quantification of Endocytosis and Macropinocytosis. Vesicle quantification by light microscopy of differential interference contrast (DIC) microscopy was performed, as previously described (8). In short, the number of vesicles above a diameter of 200 nm were quantified between experimental conditions using a combination of Zeiss (Zen) imaging software for size measurement and ImageJ for vesicle number counts using the particle counting computer-assisted program (8, 66). Thresholds were set for the DIC channels using MaxEntropy in the FIJI ImageJ software package and individual vesicles were distinguished using the binary watershed function. Particle function was applied to count number of vesicles 0.2–7 μm, circularity −1. Total number of cells counted was always more than 20 cells per experimental condition, with triplicate experiments. The sequestration of PRMT1 and GSK3 into vesicles was quantified as the colocalization using Pearson's correlation as these cytosolic proteins colocalized following Wnt-induced vesicle incorporation (8). Pearson's correlation coefficients were calculated using ImageJ software colocalization between two different channels with an $n > 20$ cells per condition, and experiments carried out in triplicate. For quantitatively analyzing BSA-DQ or TMR-dextran 70 kDa endocytosis, fluorescence was quantified in control versus treated cells using ImageJ software analyses with an $n > 25$ cells per condition. Fluorescence intensity was normalized in images compared in each condition and results from three or more independent experiments were presented as the mean ± SEM. β-Catenin nuclear localization was used as a surrogate marker for Wnt signaling activity, as it accumulates in the nucleus specifically after Wnt activation. To quantify nuclear β-catenin localization in cells treated with macropinocytosis inhibitors (EIPA and amiloride) or methyltransferase inhibitor (Adox), the first step counted the total number of cells in each condition. Next, fluorescence intensities were determined using a normalized ratio of nuclear β-catenin to cytoplasmic β-catenin. This ratio was quantified with a minimum of 25 cells per condition in triplicate samples.

Protease Protection Assay. MVB sequestration of GSK3 and PRMT1 was determined using the in situ protease protection assays as described previously (8). Cultured cells were first grown on coverslips for 24 h and treated with either Wnt3a or control medium. Subsequently, cells were placed on ice to stop endocytosis, washed twice with PBS, and permeabilized for 15–30 min in PBS containing 6.5 μg/mL digitonin. Next, cells were washed with PBS while still on ice and incubated with proteinase K (1 μg/mL) for 10 min to degrade proteins that were not sequestered in vesicles. Permeabilization with Triton X-100 was used as a control as described (8). To stop the reaction, cells were fixed in 4% PFA and analyzed by immunofluorescence.

Flow Cytometry. Cells at 70% confluency were treated with 1 mg/mL TMR-dextran diluted in prewarmed medium and incubated at 37 °C for 1 h. Cells were trypsinized, fixed in suspension with 4% (wt/vol) PFA for 15 min at room temperature, washed with DPBS, and analyzed in an LSR II flow cytometer (BD Biosciences), using the FCS Express 6 Plus (BD Biosciences) program. Fluorescence of TMR was detected by excitation at 555 nm and emission at 580 nm using the yellow-green detector.

Luciferase Assays. SW480 cells were plated on 24-well plates at 70% confluency and transfected with 1 μg of BAR DNA and 0.05 μg of Renilla reporter DNA (generous gifts from R. Moon, University of Washington, Seattle). Cells were incubated 24 h after transfection with EIPA (40 μM), amiloride (2 mM), or DMSO carrier for 2 h. Experiments were also performed with a Wnt3a-treated stably transfected HEK293T cell line (8) incubated with EIPA or amiloride for 8 h. Luciferase activity was measured with the Dual-Luciferase Reporter Assay System (Promega) according to manufacturer's instructions, using the Glomax Luminometer (Promega). Luciferase values of each sample were normalized with Renilla activity.

Statistical Analyses. Statistical analyses of computer-assisted particle analyses were performed using two-tailed *t* tests for two-sided comparisons, where statistical significance was defined as follows: $*P < 0.05$, $**P < 0.01$, and $***P < 0.001$.

ACKNOWLEDGMENTS. We thank Dr. M. Faux and the Ludwig Institute for SW480APC cells; Drs. S. Sokol, M. Bienz, R. Moon, and F. Costantini for plasmid constructs; Drs. K. Saito-Diaz and E. Lee for advice on APC siRNA; and Y. Moriyama, Y. Ding, S. Rundle, A. Dsouza, and G. Colozza for comments on the manuscript. N.T.-M. was supported by a joint University of California Institute for Mexico and the United States (UC MEXUS) and Consejo Nacional de Ciencia y Tecnología (CONACYT) postdoctoral fellowship (FE-17-65); L.V.A. was supported by an NIH postdoctoral fellowship (NIH F32 GM123622); and M.H.B. was supported by a UCLA Clinical and Translational Institute undergraduate fellowship (CTSI UL1TR000124). This work was supported by the Norman Sprague Endowment for Molecular Oncology and the Howard Hughes Medical Institute, of which E.M.D.R. is an investigator.

1. Nusse R, Clevers H (2017) Wnt/β-Catenin signaling, disease, and emerging therapeutic modalities. *Cell* 169:985–999.
2. MacDonald BT, Tamai K, He X (2009) Wnt/beta-catenin signaling: Components, mechanisms, and diseases. *Dev Cell* 17:9–26.
3. Clevers H, Nusse R (2012) Wnt/β-catenin signaling and disease. *Cell* 149:1192–1205.
4. Bilic J, et al. (2007) Wnt induces LRP6 signalosomes and promotes dishevelled-dependent LRP6 phosphorylation. *Science* 316:1619–1622.
5. Zeng X, et al. (2008) Initiation of Wnt signaling: Control of Wnt coreceptor Lrp6 phosphorylation/activation via frizzled, dishevelled and axin functions. *Development* 135:367–375.
6. Taelman VF, et al. (2010) Wnt signaling requires sequestration of glycogen synthase kinase 3 inside multivesicular endosomes. *Cell* 143:1136–1148.
7. Sahu R, et al. (2011) Microautophagy of cytosolic proteins by late endosomes. *Dev Cell* 20:131–139.
8. Albrecht LV, Ploper D, Tejeda-Muñoz N, De Robertis EM (2018) Arginine methylation is required for canonical Wnt signaling and endolysosomal trafficking. *Proc Natl Acad Sci USA* 115:E5317–E5325.
9. Acebron SP, Karaulanov E, Berger BS, Huang Y-L, Niehrs C (2014) Mitotic wnt signaling promotes protein stabilization and regulates cell size. *Mol Cell* 54:663–674.

10. Vinyoles M, et al. (2014) Multivesicular GSK3 sequestration upon Wnt signaling is controlled by p120-catenin/cadherin interaction with LRP5/6. *Mol Cell* 53:444–457.
11. Kim H, Vick P, Hedtke J, Ploper D, De Robertis EM (2015) Wnt signaling translocates Lys48-Linked polyubiquitinated proteins to the lysosomal pathway. *Cell Rep* 11:1151–1159.
12. Koch S, Acebron SP, Herbst J, Hatiboglu G, Niehrs C (2015) Post-transcriptional Wnt signaling governs epididymal sperm maturation. *Cell* 163:1225–1236.
13. Albrecht LV, Bui MH, De Robertis EM (2019) Canonical Wnt is inhibited by targeting one-carbon metabolism through methotrexate or methionine deprivation. *Proc Natl Acad Sci USA* 116:2987–2995.
14. Albrecht LV, et al. (2015) GSK3- and PRMT-1-dependent modifications of desmoplakin control desmoplakin-cytoskeleton dynamics. *J Cell Biol* 208:597–612.
15. Xu J, et al. (2013) Arginine methylation initiates BMP-induced Smad signaling. *Mol Cell* 51:5–19.
16. Katsuno Y, et al. (2018) Arginine methylation of SMAD7 by PRMT1 in TGF-β-induced epithelial-mesenchymal transition and epithelial stem-cell generation. *J Biol Chem* 293:13059–13072.
17. Clevers H (2006) Wnt/beta-catenin signaling in development and disease. *Cell* 127: 469–480.
18. Kinzler KW, Vogelstein B (1996) Lessons from hereditary colorectal cancer. *Cell* 87: 159–170.
19. Segditsas S, Tomlinson I (2006) Colorectal cancer and genetic alterations in the Wnt pathway. *Oncogene* 25:7531–7537.
20. Knudson AG (1993) Antioncogenes and human cancer. *Proc Natl Acad Sci USA* 90: 10914–10921.
21. de Lau W, Peng WC, Gros P, Clevers H (2014) The R-spondin/Lgr5/Rnf43 module: Regulator of Wnt signal strength. *Genes Dev* 28:305–316.
22. Seshagiri S, et al. (2012) Recurrent R-spondin fusions in colon cancer. *Nature* 488:660–664.
23. Saito-Diaz K, et al. (2018) APC inhibits ligand-independent Wnt signaling by the clathrin endocytic pathway. *Dev Cell* 44:566–581.e8.
24. Redelman-Sidi G, et al. (2018) The canonical Wnt pathway drives macropinocytosis in cancer. *Cancer Res* 78:4658–4670.
25. Näthke IS, Adams CL, Polakis P, Sellin JH, Nelson WJ (1996) The adenomatous polyposis coli tumor suppressor protein localizes to plasma membrane sites involved in active cell migration. *J Cell Biol* 134:165–179.
26. Nelson S, Näthke IS (2013) Interactions and functions of the adenomatous polyposis coli (APC) protein at a glance. *J Cell Sci* 126:873–877.
27. Bloomfield G, Kay RR (2016) Uses and abuses of macropinocytosis. *J Cell Sci* 129:2697–2705.
28. Buckley CM, King JS (2017) Drinking problems: Mechanisms of macropinosome formation and maturation. *FEBS J* 284:3778–3790.
29. Lewis WH (1937) Pinocytosis by malignant cells. *Am J Cancer*:666–679.
30. Doherty GJ, McMahon HT (2009) Mechanisms of endocytosis. *Annu Rev Biochem* 78: 857–902.
31. Nichols BJ, Lippincott-Schwartz J (2001) Endocytosis without clathrin coats. *Trends Cell Biol* 11:406–412.
32. Marques PE, Grinstein S, Freeman SA (2017) SnapShot:Macropinocytosis. *Cell* 169:766–766.e1.
33. Commisso C, et al. (2013) Macropinocytosis of protein is an amino acid supply route in Ras-transformed cells. *Nature* 497:633–637.
34. Recouvreux MV, Commisso C (2017) Macropinocytosis: A metabolic adaptation to nutrient stress in cancer. *Front Endocrinol (Lausanne)* 8:261.
35. Commisso C, Flinn RJ, Bar-Sagi D (2014) Determining the macropinocytic index of cells through a quantitative image-based assay. *Nat Protoc* 9:182–192.
36. Leibovitz A, et al. (1976) Classification of human colorectal adenocarcinoma cell lines. *Cancer Res* 36:4562–4569.
37. Faux MC, et al. (2004) Restoration of full-length adenomatous polyposis coli (APC) protein in a colon cancer cell line enhances cell adhesion. *J Cell Sci* 117:427–439.
38. Condon ND, et al. (2018) Macropinosome formation by tent pole ruffling in macrophages. *J Cell Biol* 217:3873–3885.
39. Capelluto DGS, et al. (2002) The DIX domain targets dishevelled to actin stress fibres and vesicular membranes. *Nature* 419:726–729.
40. Sokol SY (1996) Analysis of Dishevelled signalling pathways during Xenopus development. *Curr Biol* 6:1456–1467.
41. Itoh K, Jacob J, Sokol SY (1998) A role for Xenopus Frizzled 8 in dorsal development. *Mech Dev* 74:145–157.
42. Metcalfe C, Mendoza-Topaz C, Mieszczanek J, Bienz M (2010) Stability elements in the LRP6 cytoplasmic tail confer efficient signalling upon DIX-dependent polymerization. *J Cell Sci* 123:1588–1599.
43. Zeng L, et al. (1997) The mouse Fused locus encodes Axin, an inhibitor of the Wnt signaling pathway that regulates embryonic axis formation. *Cell* 90:181–192.
44. Bishop N, Woodman P (2000) ATPase-defective mammalian VPS4 localizes to aberrant endosomes and impairs cholesterol trafficking. *Mol Biol Cell* 11:227–239.
45. Bedford MTM, Clarke SGS (2009) Protein arginine methylation in mammals: Who, what, and why. *Mol Cell* 33:1–13.
46. Yang H, et al. (2017) Design and synthesis of novel PRMT1 inhibitors and investigation of their binding preferences using molecular modelling. *Bioorg Med Chem Lett* 27: 4635–4642.
47. Bullman S, et al. (2017) Analysis of *Fusobacterium* persistence and antibiotic response in colorectal cancer. *Science* 358:1443–1448.
48. Reilein A, Nelson WJ (2005) APC is a component of an organizing template for cortical microtubule networks. *Nat Cell Biol* 7:463–473.
49. Yamamoto H, Komekado H, Kikuchi A (2006) Caveolin is necessary for Wnt-3a-dependent internalization of LRP6 and accumulation of beta-catenin. *Dev Cell* 11: 213–223.
50. Blitzer JT, Nusse R (2006) A critical role for endocytosis in Wnt signaling. *BMC Cell Biol* 7:28.
51. McKanna JA, Haigler HT, Cohen S (1979) Hormone receptor topology and dynamics: Morphological analysis using ferritin-labeled epidermal growth factor. *Proc Natl Acad Sci USA* 76:5689–5693.
52. Haigler HT, McKanna JA, Cohen S (1979) Rapid stimulation of pinocytosis in human carcinoma cells A-431 by epidermal growth factor. *J Cell Biol* 83:82–90.
53. Yoshida S, Pacitto R, Inoki K, Swanson J (2018) Macropinocytosis, mTORC1 and cellular growth control. *Cell Mol Life Sci* 75:1227–1239.
54. Palm W, Thompson CB (2017) Nutrient acquisition strategies of mammalian cells. *Nature* 546:234–242.
55. Pate KT, et al. (2014) Wnt signaling directs a metabolic program of glycolysis and angiogenesis in colon cancer. *EMBO J* 33:1454–1473.
56. Thompson CB (2014) Wnt meets Warburg: Another piece in the puzzle? *EMBO J* 33: 1420–1422.
57. Crosignani V, et al. (2012) Deep tissue fluorescence imaging and in vivo biological applications. *J Biomed Opt* 17:116023.
58. Matsuda H, Shi Y-B (2010) An essential and evolutionarily conserved role of protein arginine methyltransferase 1 for adult intestinal stem cells during postembryonic development. *Stem Cells* 28:2073–2083.
59. Pavlova NN, Thompson CB (2016) The emerging hallmarks of cancer metabolism. *Cell Metab* 23:27–47.
60. Chapman-Andresen C, Holter H (1955) Studies on the ingestion of ^{14}C glucose by pinocytosis in the amoeba Chaos chaos. *Exp Cell Res* 3:52–63.
61. Acebron SP, Niehrs C (2016) β-Catenin-Independent roles of Wnt/LRP6 signaling. *Trends Cell Biol* 26:956–967.
62. Bar-Sagi D, Feramisco JR (1986) Induction of membrane ruffling and fluid-phase pinocytosis in quiescent fibroblasts by ras proteins. *Science* 233:1061–1068.
63. Palm W, et al. (2015) The utilization of extracellular proteins as nutrients is suppressed by mTORC1. *Cell* 162:259–270.
64. Palm W, Araki J, King B, DeMatteo RG, Thompson CB (2017) Critical role for PI3-kinase in regulating the use of proteins as an amino acid source. *Proc Natl Acad Sci USA* 114: E8628–E8636.
65. West MA, Bretscher MS, Watts C (1989) Distinct endocytotic pathways in epidermal growth factor-stimulated human carcinoma A431 cells. *J Cell Biol* 109:2731–2739.
66. Arena ET, et al. (2017) Quantitating the cells: Turning images into numbers with ImageJ. *WIREs Dev Biol* 6:e260.